Estimation of speed and direction of arm movements from M1 activity using a nonlinear neural decoder

Jisung Park
Department of Human Factors Engineering
Ulsan National Institute of Science and Technology
Ulsan, Republic of Korea
teran0729@unist.ac.kr

Sung-Phil Kim
Department of Human Factors Engineering
Ulsan National Institute of Science and Technology
Ulsan, Republic of Korea
spkim@unist.ac.kr

***Abstract*— The current neural decoding algorithms for brain-machine interfaces (BMIs) have largely focused on predicting the velocity of arm movements from neuronal ensemble activity. Yet, mounting evidence indicates that velocity is encoded separately in motor cortical activity. In this regard, we aimed to decode separate speed and direction information independently using a machine learning algorithm based on long short-term memory (LSTM). The performance of the proposed decoder was compared with the traditional decodres using velocity Kalman filter and the velocity LSTM. The proposed decoder showed better angular prediction than the other decoders. Also, the reconstruction hand trajectories with the proposed decoder acquired the targets more often. Movement time of the reconstructed trajectories by the proposed decoder was shorter than the others. Our results suggest advantages of decoding speed and direction independently using a nonlinear model such as LSTM for intracortical BMIs.**

Brain Machine Interfcace, Primary motor cortex, Decoding, Long short-term memory

I. Introduction

Brain machine interfaces (BMI) offer a direct pathway between neural signals of the user and targeted external devices such as a robot arm or wheel chair. To control the devices, especially the robot arm, elaborated algorithms extracting intended kinematic information

from neural signals have widely been developed. One of the algorithms, Kalman filter (KF), has been suggested as a neural decoder for controlling an actuator by harnessing neural activity [1]. In addition to such linear algorithms, nonlinear prediction algorithms have also been suggested. Li *et al*. estimated the hand position and velocity from neuronal ensemble signals with the unscented Kalman filter, which a nonlinear variant of KF [2]. Also, Xu *et al*. compared general regression neural network (GRNN) and support vector regression (SVR) with the linear Kalman filter for neural decoding and showed better performance of nonlinear decoders [3]. Recently, deep learning methods such as long short-term memory (LSTM) were compared with traditional decoding algorithms for neural decoding [4]. All these algorithms estimating arm movements have primarily focused on predicting velocity.

Nonetheless, there have been mounting evidence showing that kinematic variables of speed and direction are encoded differently in the motor cortex. Golub *et al*. showed that directional information is more dominantly encoded than the speed information in the motor cortex during arm movements when measured in a specific time window, implying that the speed information should be decoded with a more robust means [5].

Thus, in this study, we assumed that separate decoding of speed and direction, instead of velocity, would yield more accurate estimation of arm kinematic variables. Under the consideration of nonlinear relations between neural activity and the kinematic variables, we designed a decoding algorithm consisting of dual models of LSTM predicting speed and direction independently, which we called speed-direction LSTM (*sd*LSTM). The proposed decoding algorithm was compared with the velocity Kalman filter and the velocity LSTM that have been proposed before.

This research was supported by the Brain Research Program through the National Research Foundation of Korea (NRF) funded by the Ministry of Science, ICT & Future Planning (2016M3C7A1904988).

II. Data description

We analyzed behavioral and neural data in a non-human primate recorded during the center-out task, provided in the public dataset by the Collaborative Research in Computational Neuroscience (CRCNS) [6]. In the task, one of the eight targets radially located at a distance from a home position at the center of the screen with a 45-degree angle interval was given randomly in each trial (Fig. 1). The distance between home and the target was 10 cm. A trial was regarded as a success when

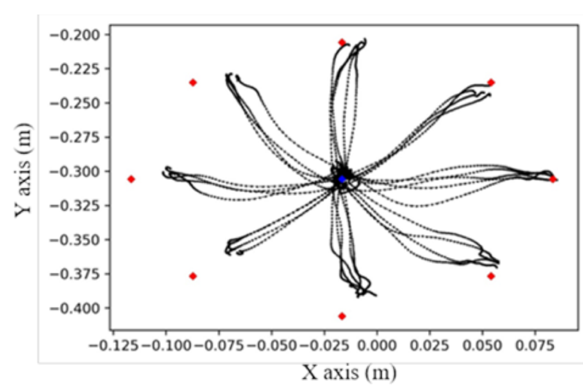

Figure 1. Trajectory example of center-out task. The red dot represents the positions of eight target and the blue dot at the center of the screen indicates the home position.

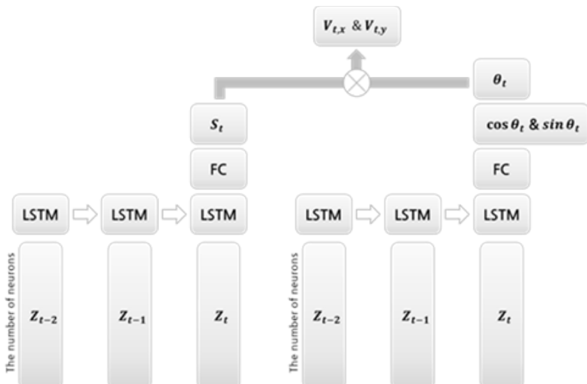

Figure 2. The design of speed-direction LSTM

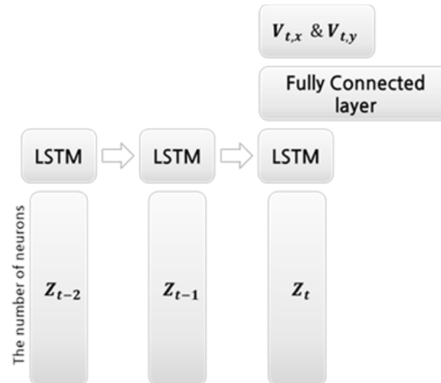

Figure 3. The design of velocity LSTM

the cursor moved by the subject dwelled on a square of 2 x 2 cm^2 around the target position. In each trial, the subject should hold the cursor at the home position for 0.5 ~ 0.6 s. When the target cue was given, the subject moved the cursor toward the target and held it over the target for 0.2 ~ 0.4 s to acquire the target. A total of 194 trials were performed by the subject among which we analyzed 175 successful trials. 60 % of the trials was used for training the decoding algorithm, 20 % for validation and 20% for test. No cross-validation was employed here to follow a general BMI paradigm.

A total of 196 neurons were detected with the silicon microelectrode array (96-channel, Blackrock, Inc., USA), implanted in the primary motor cortex (M1). Among the recorded neurons, we only explored 158 neurons excluding those neurons that fired rarely during the task. The neuronal firing rate was estimated by the number of spikes in the time bin of 50 ms, without overlapping between the time bins. Three consecutive bins were used as input to the decoders.

III. Methods

A. Decoding algorithms

We designed the neural decoder predicting the speed and direction separately of endpoint movement of the arm with LSTM and merging the estimated speed and direction into a velocity vector (*sd*LSTM) (Fig. 2). Each pat of *sd*LSTM received preprocessed neural data as input vectors with the sequence length of 3 (i.e. 150 ms). The time series data was transformed into the hidden states in the LSTM cell and transferred to the fully connected (FC) layer, followed by the output unit, which generated the estimates of the movement speed and direction at time *t*. For the estimation of the movement direction, the cosine and sine functions of directional angle were decoded separately instead of directly estimating an angle in radian because of the periodicity.

The velocity LSTM (*v*LSTM) predicted x-, and y-coordinates of the hand velocity at time *t* from the same sequence of neural ensemble activity (Fig. 3). Its structure was designed in a similar way with the previous study [4]. Both *sd*LSTM and *v*LSTM updated the weights with the mean squared loss and optimaled the weight sets with the Adam optimizer and random search [7,8].

The velocity Kalman filter (*v*KF) consisted of the prediction step and the correction step. The prediction step represented a linear relation between kinematic variables over time. The correction step rectified the predicted kinematic states from the observation of neural activity (Eqs 1,2).

$$Z_k = H_k X_k + q_k \tag{1}$$

$$X_{k+1} = A_k X_k + w_k \tag{2}$$

In Eq. 1, which is the correction step, Z_k is the observed firing rates of 158 neurons concatenated over three bins. X_k is the hand velocity and H_k represents how the kinematic variable is encoded in the firing rate. Eq. 2 indicates the prediction step. A_k links the state at time *k* to that at time *k*+1. q_k and w_k are noise assumed to follow the normal distribution with zero mean and a covariance matrix Q_k and W_k, respectively. The detailed illustration is described in [1].

B. Measurement index

We assess the quality of the reconstructed trajectory by decoding algorithms using three indices. First, the angular difference (AD) between the reconstructed and true movement direction was measured. It indicates how consistently the decoded arm movements moves to the target similar to the true trajectory. It was obtained with the equation (3) and (4).

$$AD = \frac{1}{n}\sum_{t=0}^{n} \theta_t \tag{3}$$

$$\theta_t = \cos^{-1} \frac{V_t \cdot \hat{V}_t}{|V_t||\hat{V}_t|} \tag{4}$$

V_t represents the velocity vector of actual arm movement and the $\hat{V}_t$ is a reconstructed velocity vector at time *t*. The angular differences of each trial were averaged. To compare the index among the decoders, one-way repeated measure ANOVA was used. The post hoc test was performed to evaluate a difference between each pair of decoders.

Second, we measured how frequently the reconstructed trajectory reached the target, denoted as a hit rate. It represents

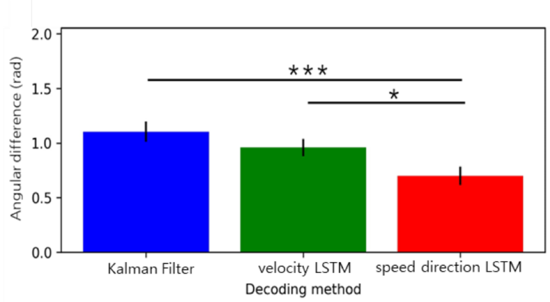

Figure 4. Averaged angular difference of each neural decoders. The significant difference between decoders was marked as asterisk.

how successively the decoded trajectory was formed enough to acquire the target.

Finally, we measured the distance to the target of the reconstructed position of endpoints according to the task time. It shows how efficiently the decoded trajectory reached the target. We acquired the distance for every 10 % of each trial time because every trial had different time lengths.

IV. Results

The averaged angular difference was 1.104 ± 0.094, 0.9587 ± 0.081 and 0.6994 ± 0.0852 rad for *v*KF, *v*LSTM and *sd*LSTM, respectively (Fig. 4). One-way repeated measures ANOVA revealed that there was the effect of decoder type on the angular difference ($F(2, 68) = 12.683$, $p < 0.001$). The *post hoc* test, corrected with Bonferroni, identified that there was no difference between *v*KF and *v*LSTM ($p = 0.1354$). On the other hand, *sd*LSTM showed significantly smaller angle differences compared with *v*KF and *v*LSTM ($p < 0.05$).

Fig. 5 shows changes in distance to the target as the task time was elapsed. When the task was finished, the averaged distance (bold line in the figure) by actual movements was 0.012 ± 8.56×10^{-4}. One-way repeated measures ANOVA was performed on distance to the target at 100 % of the progress time of each trials from all the decoders. It revealed the effect

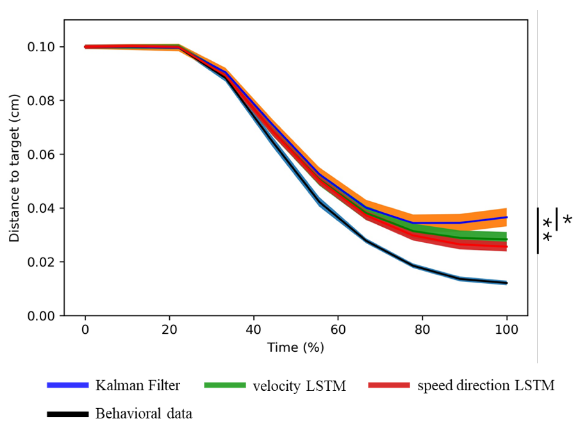

Figure 5. Averaged Distance to target according to task time. The significant difference between decoders was marked as asterisk.

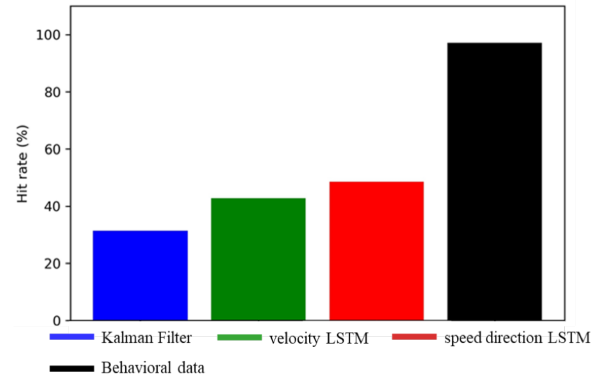

Figure 6. Averaged hit rate of each neural decoders

of decoder type on distance ($F(2,68) = 8.556$, $p < .001$). The *post hoc* tests showed that there was a significant difference between *v*KF (M = 0.0366, SE = 0.0034) and *v*LSTM (M = 0.284, SE = 0.0028) ($p < .05$). Also, there was a significant difference between vKF and *sd*LSTM (M = 0.0256, SE = 0.0018) ($p < 0.01$). Note that distance to the target of *v*KF increased after 80 % of the trial time because most of the reconstructed trajectory passed the target.

Fig. 6 shows the hit rate of each decoder. The hit rate was 31.88, 43.13 and 48.13% for *v*KF, *v*LSTM and *sd*LSTM, respectively. It showed that *sd*LSTM achieved the highest hit rate.

V. Conclusion

In this study, we proposed a novel decoder that prediced speed and direction of the hand separately with dual LSTM models. The proposed decoder improved the prediction of movement direction compared with the velocity Kalman filter and the velocity LSTM. Also, it reconstructed hand trajectories better than other decoders. Achievement of higher decoding performance by separating speed and direction instead of targeting velocity may support that the encoding of speed and direction could be distinguishable in the motor cortical activity.

References

[1] Wu, W., Black, M. J., Gao, Y., Serruya, M., Shaikhouni, A., Donoghue, J. P., & Bienenstock, E. (2003). Neural decoding of cursor motion using a Kalman filter. In *Advances in neural information processing systems* (pp. 133-140).

[2] Li, Z., O'Doherty, J. E., Hanson, T. L., Lebedev, M. A., Henriquez, C. S., & Nicolelis, M. A. (2009). Unscented Kalman filter for brain-machine interfaces. *PloS one*, *4*(7), e6243.

[3] Xu, K., Wang, Y., Zhang, S., Zhao, T., Wang, Y., Chen, W., & Zheng, X. (2011, August). Comparisons between linear and nonlinear methods for decoding motor cortical activities of monkey. In *Engineering in Medicine and Biology Society, EMBC, 2011 Annual International Conference of the IEEE* (pp. 4207-4210). IEEE.

[4] Glaser, J. I., Chowdhury, R. H., Perich, M. G., Miller, L. E., & Kording, K. P. (2017). Machine learning for neural decoding. *arXiv preprint arXiv:1708.00909*.

[5] Golub, M. D., Yu, B. M., Schwartz, A. B., & Chase, S. M. (2014). Motor cortical control of movement speed with implications for brain-machine interface control. Journal of neurophysiology, 112(2), 411-429.

[6] Flint, R. D., Lindberg, E. W., Jordan, L. R., Miller, L. E., & Slutzky, M. W. (2012). Accurate decoding of reaching movements from field

potentials in the absence of spikes. *Journal of neural engineering*, *9*(4), 046006.

[7] Kingma, D. P., & Ba, J. (2014). Adam: A method for stochastic optimization. arXiv preprint arXiv:1412.6980.

[8] Bergstra, J., & Bengio, Y. (2012). Random search for hyper-parameter optimization. Journal of Machine Learning Research, 13(Feb), 281-305